

Polymerizable AEE-active Dye with Optical Activity for Fluorescent Nanoparticles Based on Phenothiazine: Synthesis, Self-assembly and Biological Imaging

Zeng-Fang Huang^{a,b*}, Ya-Li Chen^{a,b}, Chao-Yue Zhou^{a,b}, Yan-Hong Li^a, Mei Li^a, Xiao-Bo Liu^b, Liu-Cheng Mao^c, Jin-Ying Yuan^c, Lei Tao^c, and Yen Wei^{c*}

^a School of Materials & Food Engineering, Zhongshan Institute, University of Electronic Science & Technology of China, Zhongshan 528402, China

^b School of Materials and Energy, University of Electronic Science & Technology of China, Chengdu 610054, China

^c Department of Chemistry, the Tsinghua Center for Frontier Polymer Research, Tsinghua University, Beijing 100084, China

Electronic Supplementary Information

Abstract In consideration of various advantages such as less harm, higher sensitivity, and deeper imaging depth, etc., AIE materials with long-wave emission are attracting extensive attention in the fields of vascular visualization, organelle imaging, cells tracker, forensic detection, bioprobe and chemosensor, etc. In this work, a novel fluorescent (*R*)-PVHMA monomer with chirality and aggregation-induced emission enhancement (AEE) characteristics was acquired through enzymatic transesterification reaction basing on phenothiazine, and its $[\alpha]_D^{25^\circ C}$ value was about -6.39° with a 3.08 eV bandgap calculated by the quantum calculations. Afterwards, a series of PEG-PVH1 and PEG-PVH2 copolymers with chirality feature were achieved through RAFT polymerization of the obtained (*R*)-PVHMA and PEGMA with various feed ratios. When the feed molar ratio of (*R*)-PVHMA increased from 21.5% to 29.6%, its actual molar fractions in the PEG-PVH1 and PEG-PVH2 copolymers accordingly increased from 18.1% to 25.7%. The molecular weight of PEG-PVH1 was about 2.2×10^4 with a narrow PDI, and their kinetics estimation showed a first-order quasilinear procedure. In aqueous solution, the amphiphilic copolymers PEG-PVH could self-assemble into about 100 nm nanoparticles. In a 90% water solution of H₂O and THF mixture, the fluorescence intensity had the maximum value, and the emission wavelength presented at 580 and 630 nm. The investigation of cytotoxicity and cells uptake showed that PEG-PVH FONs performed outstanding biocompatibility and excellent cells absorption effects, which have great potential in bioimaging application.

Keywords AEE dye; Optical activity; RAFT polymerization; Long-wave emission; Biological imaging

Citation: Huang, Z. F.; Chen, Y. L.; Zhou, C. Y.; Li, Y. H.; Li, M.; Liu, X. B.; Mao, L. C.; Yuan, J. Y.; Tao, L.; Wei, Y. Polymerizable AEE-active dye with optical activity for fluorescent nanoparticles based on phenothiazine: synthesis, self-assembly and biological imaging. *Chinese J. Polym. Sci.* 2021, 39, 1431–1440.

INTRODUCTION

AIE materials with long-wave emission are attracting people's extensive attention and interest in many fields due to their various advantages such as less harm, higher sensitivity, and deeper imaging depth, etc.^[1–7] Heterocyclic compounds of five- or six-membered rings have been extensively studied since their discovery. The heteroatoms have also evolved from the original O, N and S atoms to a variety of metallic and non-metallic atoms, and the application of these heterocyclic compounds extends to bioengineering, bioimaging, dye chemistry and many other fields. A large proportion of these heterocyclic compounds can emit fluorescence with long-wave

emission, such as phenothiazine, benzothiadiazole and organo-boron compounds, etc., so they are widely used as organic fluorescent materials in organic optoelectronic devices, fluorescence chemical analysis, biomedical tracer and so on.^[8–15] For example, benzo-2,1,3-thiadiazole moieties can also strongly shift the emission wavelength from blue to red with adjusting the fluorescence characteristics of aggregation-enhanced emission.^[16] PIPBT-TPE and PITBT-TPE with N and S atoms heterocyclic rings can emit green fluorescence at 560 nm and red fluorescence at 645 nm, and they were applied for real-time fluorescence *in vivo* blood visualization due to the excellent biocompatibility and prospective candidates for living cells and tissue imaging.^[17] BTD-TPA and BTD-NPA red luminogens with benzothiadiazole and arylamino moieties showed aggregation-induced emission (AIE) features with about 600 nm emission wavelength, which could be used as important biomolecules for sensitive detection of dopamine (DA) with high selectivity.^[18] Another pH-sensitive fluorescent probe of imidazole-fused

* Corresponding authors, E-mail: hzf105@163.com (Z.F.H.)

E-mail: weiyen@tsinghua.edu.cn (Y.W.)

Received February 9, 2021; Accepted April 20, 2021; Published online July 8, 2021

benzothiadiazole was synthesized with the excellent fluorescence properties and lysosomal targeting ability, and it has been successfully used to monitor the pH variety in lysosomes which were induced by Baf-A1 or chloroquine.^[19] Similarly, a new class of phenanthroimidazole-based organic boron compounds have been synthesized. Their solution-state fluorescence quantum yields range from 0.07 to 0.88, and their solid-state quantum yields are moderate, which are used in organic light-emitting diodes and fluorescent probes.^[20]

The phenothiazine with the heteroatomic six-membered ring has a bifacial angle of 153°, presenting a twisted butterfly-like structure, which makes itself both rigid and flexible. At the same time, phenothiazine has a relatively strong electron-donating ability, and its introduction into the molecular structure can reduce the energy level difference between the highest occupied molecular orbital (HOMO) and the lowest unoccupied molecular orbital (LUMO), making the emission wavelength of the molecule increase, and can be used as an electron donor (D) to construct D-A fluorescent molecules with red light emission.^[21–23] For example, a series of novel phenothiazine chalcone derivatives were constructed with the D- π -A structure and low band gap energy, and they had obvious red emission, aggregation-induced emission enhancement (AEE) characteristics and reversible "turn-on" mechanofluorochromism behavior, which made them potential candidates for the manufacture of color-changing switches and piezoelectric smart optoelectronic devices.^[24] Moreover, a series of new derivatives of PEGylated phenothiazines were produced by grafting PEGMA to phenothiazine, which could assemble to form submicrometric aggregates and induce fluorescence emission due to the good solubility and hydrolytic stability. These derivatives not only retained the potential for the preparation of biological materials, but also could be applied in the field of optoelectronics.^[25]

Chirality is a ubiquitous feature in nature and organisms, involving a wide range from small molecules to large molecules, and nature seems to have a selective preference for the chirality of specific molecules. Almost all the amino acids that make up the lives of the earth are levorotatory, while the sugar units and DNA in sugars and nucleic acids are dextrorotatory. The ingenious design contains philosophy: different enantiomers of the same molecule often have very different effects on the organism, which makes the feature of chirality be vital in life science and biomedicine. With the vigorous development in the areas of life sciences, medicine, and chemistry science, researches on understanding and exploration of opponent molecules are also deepening with extensive achievements.^[26–30] The first Nobel prize of chemistry in the 21st century was awarded to chirality catalysis. In recent years, due to the superior performance of the polymer itself, chirality research has gradually extended to chiral polymers, which have prospective applications in the areas of chiral recognition, racemic separation, asymmetric synthesis, chiral catalysis, liquid crystal, drug synthesis, etc.^[31–36]

In consideration of the excellent fluorescence and long-wave emission property of phenothiazine in the aggregated state, in this study, a novel polymerizable fluorescent (*R*)-PVHMA dye with AEE and chirality features was acquired

through Suzuki coupling reaction and enzymatic transesterification using phenothiazine as the basic skeleton. The obtained (*R*)-PVHMA monomer has a specific rotation $[\alpha]_D^{25}$ of -6.39° with excellent red-yellow fluorescence emission, which is desirable for cells imaging. Afterwards, a series of PEG-PVH1 and PEG-PVH2 fluorescent copolymers having chirality were further prepared by (*R*)-PVHMA monomer and hydrophilic monomer PEGMA via RAFT polymerization with a quasilinear first-order procedure, which could be easily self-assembled into nanoparticles in water. The estimation of cytotoxicity and cell uptake behavior shows that PEG-PVH nanoparticles present outstanding biocompatibility and cells internalization effect, which have promising potential in bioimaging area.

EXPERIMENTAL

Materials and Characterization

1-Bromooctadecane (Aladdin, 97%), potassium *tert*-butanol (Aladdin, 95%), phosphoryl chloride (Xiya Reagent Co., Ltd., 99%), 2,2,2-trifluoroethyl methacrylate (TFEMA) (Aladdin, 98%), 6-chloro-2-hexanone (Aladdin, 97%), tetrabutylammonium-hydroxide solution (TBAH) (Aladdin, ~25% in methanol, ~0.8 mol/L), phenothiazine (Aladdin, 98%), sodium iodide, 1,2-dichloroethane (Aladdin, 99.8%), 4-hydroxyphenylacetone nitrile (Aladdin, 98%), 2,2-azobisisobutyronitrile (AIBN) (Aladdin, 99%), Novozym 435, potassium carbonate, triethylamine (TEA) and sodium bicarbonate were purchased directly for use. Poly(ethylene glycol) monomethacrylate (PEGMA) (Aladdin, $M_n=475$, AR) was purified through an aluminum oxide column before use. The solvents such as *n*-hexane, methylene chloride, etc. used directly in the experiment were analytical reagent. 6-Chloro-2-hexanol (CHOL), 10-octadecyl-10*H*-phenothiazine-3-carbaldehyde (OPC) and chain transfer agent (CTA) of 4-cyano-4-(ethylthiocarbonothioylthio) pentanoic acid were self-made in the laboratory according to the reported references.^[37–40]

The chemical structure of the target products was determined by hydrogen spectroscopy of nuclear magnetic resonance (¹H-NMR) and Fourier transform infrared (FTIR) spectroscopy. The ¹H-NMR spectroscopy was measured on a JEOL JNM-ECA 400 (400 MHz) spectrometer with chloroform (CDCl₃) as the solvent and tetramethylsilane (TMS) as the reference. Infrared spectra were acquired on a PerkinElmer TWO spectrometer. The molecular weight (M_n , g/mol) and the polydispersity index (PDI) were obtained from a gel permeation chromatograph (GPC) model of a Waters 1515 equipment using tetrahydrofuran (THF) as mobile phase at 1.0 mL/min flow rate. Transmission electron microscopy (TEM) images of copolymer nanoparticles were obtained on a transmission electron microscope model of JEM-1200EX at an operating voltage of 100 kV. The preparation process of the test sample was as follows: 10 mg of the target copolymers were added into 4 mL of deionized water and dissolved completely, and then added a drop of mixed solution onto the carbon-coated copper grids and let it stand until dry. Ultraviolet-visible spectra (UV-Vis) were recorded on a Perkin-Elmer LAMBDA 35 spectrophotometer. The fluorescence curves were acquired on a Hitachi F-2700 spectrophotometer. The specific rotation of the (*R*)-PVHMA monomer and PEG-PVH was measured

red on an SGW-3 autopolarizer in acetone (concentration=10 mg/mL) at 25 °C.

Synthesis of 2-(4-((5-Hydroxyhexyl)oxy)phenyl)acetonitrile (HPA)

4-Hydroxyphenylacetonitrile (1.13 g, 8.5 mmol), CHOL (1.50 g, 11.0 mmol), potassium carbonate (2.93 g, 21.25 mmol), sodium iodide (140 mg), DMF (35.0 mL) and a magnetic stir bar were added into a Schlenk tube, and then this tube was sealed, frozen in liquid nitrogen and deoxidized for five times of vacuum-nitrogen cycles. The Schlenk tube was then heated and stirred at 100 °C for 24 h in an oil bath. Afterwards, the pH was neutralized to 4–5 with 3 mol/L of hydrochloric acid. An appropriate amount of distilled water was put into the Schlenk tube, and then the organic phase was extracted for three times using ethyl acetate and dried with anhydrous MgSO_4 . The reaction mixture was further filtered to remove MgSO_4 , and the crude product was acquired through removing the solvent on a rotary evaporator. The product was further purified on a silica column using petroleum ether/ethyl acetate ($V/V=1/1$) as mobile phase, and the pure product HPA was obtained after completely drying under vacuum (1.61 g, 81%). $^1\text{H-NMR}$ (400 MHz, CDCl_3 , δ , ppm): 1.23–1.24 (d, $J=4.0$ Hz, 3H; CH_3), 1.53–1.56 (m, 4H; $-\text{CH}_2-$), 1.60–1.64 (m, 1H; $-\text{OH}$), 1.81–1.85 (m, 2H; $-\text{CH}_2-$), 3.70 (s, 2H; $-\text{CH}_2\text{CN}$), 3.84–3.88 (m, 1H; $-\text{CH}$), 3.97–4.00 (t, $J=6.0$ Hz, 2H; $-\text{CH}_2\text{Cl}$), 6.89–6.91 (d, $J=6.0$ Hz, 2H; ArH), 7.23–7.25 (d, $J=8.0$ Hz, 2H; ArH).

Synthesis of (R)-6-(4-(Cyanomethyl)phenoxy)hexan-2-yl Methacrylate ((R)-PHMA)

Novozym435 (294 mg) and a magnetic stir bar were added into a Schlenk tube, and then this tube was sealed and deoxidized for five times by vacuum-nitrogen cycling. HPA (1.63 g, 7.0 mmol), TFEMA (0.71 g, 4.2 mmol) and TEA (0.35 g, 3.5 mmol) were completely dissolved in toluene (20.0 mL), followed by injection of the mixture into the Schlenk tube, which was put into an oil bath at 55 °C and stirred for 24 h. Subsequently, Novozym435 catalytic agent was eliminated through centrifugation, and then the solvent of the crude product was eliminated through a rotary evaporator. Finally, the product was purified through a silica column taking petroleum ether/ethyl acetate ($V/V=2/1$) as eluent, and the product (R)-PHMA was obtained by drying under vacuum (0.66 g, 63%). $^1\text{H-NMR}$ (400 MHz, CDCl_3 , δ , ppm): 1.28–1.30 (d, $J=8.0$ Hz, 3H; $-\text{CH}_3$), 1.50–1.70 (m, 4H; $-\text{CH}_2-$), 1.77–1.84 (m, 2H; $-\text{CH}_2-$), 1.96 (s, 3H; $-\text{CH}_3$), 3.70 (s, 2H; $-\text{CH}_2\text{CN}$), 3.95–3.98 (t, $J=6.0$ Hz, 2H; $-\text{CH}_2\text{Cl}$), 5.00–5.04 (m, 1H; $-\text{CH}$), 5.56 (s, 1H; $-\text{CH}$), 6.10 (s, 1H; $-\text{CH}$), 6.89–6.90 (d, $J=4.0$ Hz, 2H; ArH), 7.23–7.25 (d, $J=8.0$ Hz, 2H; ArH).

Synthesis of (R)-6-(4-(1-Cyano-2-(10-octadecane-10H-phenothiazin-3-yl)vinyl)phenoxy)hexan-2-yl methacrylate ((R)-PVHMA)

OPC (1.16 g, 2.42 mmol), (R)-PHMA (0.66 g, 2.2 mmol), TBAH (5–6 drops), ethanol (20.0 mL) and a magnetic stir bar were put into a Schlenk tube, and then this tube was stirred magnetically for 0.5 h at 30 °C to make the mixture completely dissolve. The Schlenk tube was then heated and stirred for 5 h at 78 °C. At the end of the reaction, the product was obtained by removing the solvent on a rotary evaporator, which was further purified through a silica column taking dichloromethane/*n*-hexane

($V/V=2:1$) as eluent, and the pure product (R)-PVHMA was dried under vacuum (1.00 g, 60%). $^1\text{H-NMR}$ (400 MHz, CDCl_3 , δ , ppm): 0.88–0.92 (t, $J=8.0$ Hz, 3H, $-\text{CH}_3$), 1.20–1.34 (m, 29H, $-\text{C}_{13}\text{H}_{26}-$, $-\text{CH}_3$), 1.42–1.48 (m, 2H, $-\text{CH}_2-$), 1.52–1.67 (m, 6H, $-\text{CH}_2-$), 1.80–1.87 (m, 4H, $-\text{CH}_2-$), 1.97 (s, 3H, $-\text{CH}_3$), 3.90 (s, 2H, $-\text{CH}_2-$), 4.00–4.03 (t, $J=6.0$ Hz, 2H, $-\text{CH}_2\text{Cl}$), 5.00–5.04 (m, 1H, $-\text{CH}$), 5.56 (s, 1H, $-\text{CH}$), 6.11 (s, 1H, $-\text{CH}$), 6.88–6.89 (d, $J=4.0$ Hz, 2H, ArH), 6.93–6.95 (d, $J=8.0$ Hz, 3H, ArH), 7.14 (m, 2H, ArH), 7.32–7.34 (d, $J=4.0$ Hz, 1H, ArH), 7.55 (s, 1H, Ar-CH), 7.56–7.58 (d, $J=8.0$ Hz, 2H, ArH), 7.80–7.82 (d, $J=8.0$ Hz, 1H, ArH). $^{13}\text{C-NMR}$ (400 MHz, CDCl_3 , Fig. S1 in the electronic supplementary information, ESI): 14.13, 17.93, 19.97, 21.31, 22.01, 22.70, 26.94, 29.67, 31.89, 35.75, 67.94, 70.86, 115.00, 124.73, 127.37, 137.11. The molecular weight by TOFMS=762.5 (Fig. S2 in ESI).

Synthesis of PEG-PVH Amphiphilic Copolymers

(R)-PVHMA (104.3 mg, 0.137 mmol), AIBN (1.0 mg, 0.006 mmol), PEGMA (237 mg, 0.499 mmol), CTA (3.1 mg, 0.012 mmol), toluene (2.0 mL) and a magnetic stir bar were placed into a Schlenk tube, subsequently, this tube was sealed, frozen in liquid N_2 and then deoxygenated by vacuum-nitrogen cycles for five times. The Schlenk tube was then heated and stirred at 70 °C for 36 h. After the reaction was completed, the mixture was continually dialyzed with acetone for three times for 12 h each. The crude product was obtained by removing the organic solvent on a rotary evaporator, and then purified by multiple cycles of tetrahydrofuran dissolution and petroleum ether precipitation, and the resulted PEG-PVH1 copolymers were dried under vacuum with the yield of 0.26 g. Another PEG-PVH2 copolymers were fabricated according to the same method as described above, where the molar ratio of (R)-PHMA was adjusted to 29.6%, yield: 0.27 g.

RESULTS AND DISCUSSION

Characterization and Features of PEG-PVH FONS

Scheme 1 shows the synthetic route to the fluorescence monomer (R)-PVHMA and this process can be divided into three parts. Firstly, the nucleophilic substitution reaction of phenothiazine (PHT) and 1-bromooctadecane was used to obtain the intermediate product 10-octadecanephenothiazine (OPHT), which was followed by a Vilsmeier-Haack reaction with DMF catalyzed by phosphoryl chloride to obtain the OPC. Secondly, HPA was obtained by the nucleophilic substitution reaction of 4-hydroxyphenylacetonitrile and CHOL, and it would continually perform the transesterification reaction with TEFMA catalyzed by Novozym435 to obtain chiral molecule (R)-PHMA with *R* conformation through the efficient chiral resolution of racemic secondary alcohol. Thirdly, the aldehyde group in the OPC structure will undergo a Knoevenagel condensation reaction with the active methylene of (R)-PHMA and obtain the chiral fluorescence monomer (R)-PVHMA. Subsequently, the RAFT polymerization of (R)-PVHMA with PEGMA was used to prepare the corresponding amphiphilic PEG-PVH copolymers with chirality property, which tended to self-assemble into nanoparticles due to their amphiphilicity and could be easily absorbed by cells, as exhibited in Scheme 2.

The GPC data for the target PEG-PVH1 copolymers was exhibited in Fig. 1(A), the M_n value was about 2.2×10^4 , and their

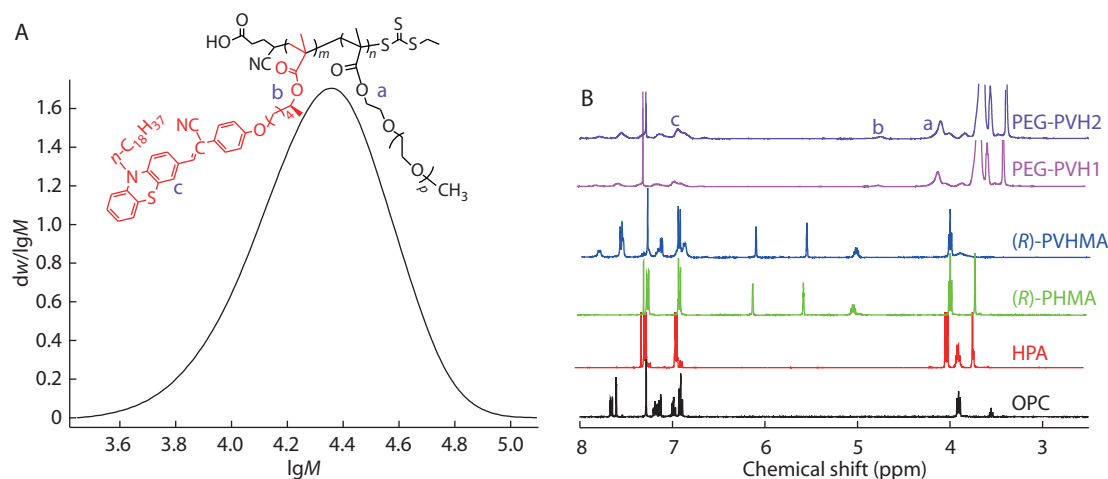


Fig. 1 (A) GPC curve of PEG-PVH1; (B) $^1\text{H-NMR}$ spectra (CDCl_3) of OPC, HPA, (*R*)-PHMA, fluorescent (*R*)-PVHMA dye and fluorescent PEG-PVH copolymers.

the Knoevenagel condensation reaction of aldehyde group and active methylene group, which connected OPC and (*R*)-PHMA through a $\text{C}=\text{C}$ bond. For the $^1\text{H-NMR}$ spectrum of (*R*)-PVHMA, the peak at 3.70 ppm assigned to the $-\text{CH}_2-\text{CN}$ disappeared completely, while the characteristic proton peaks at 3.98, 5.02, 5.56 and 6.10 ppm were unchanged, in addition, the peak of $-\text{CH}_2-$ linking to the N atom still appeared at 3.90 ppm, and these results implied the successful Knoevenagel condensation reaction between OPC and (*R*)-PHMA. Basing on RAFT polymerization of (*R*)-PVHMA and PEGMA, the $-\text{C}=\text{CH}_2$ double bonds in the structure were broken and the characteristic proton peaks at 5.56 and 6.10 ppm assigned to $-\text{C}=\text{CH}_2$ completely disappeared. At the same time, the electron density of the H atom bonding to the chiral C atom increased slightly, and its characteristic peak shifted slightly towards the high field, appearing at 4.75 ppm. The peaks of methylene $-\text{CH}_2-$ linking to the ester group in the PEGMA were presented at 4.10 ppm, and the typical peaks of aromatic rings in (*R*)-PVHMA at 6.90–7.80 ppm. The disappearance of the peaks at 5.56 and 6.10 ppm implied that (*R*)-PVHMA and PEGMA polymerized successfully into the PEG-PVH copolymers through RAFT polymerization. A rough estimation demonstrated that the molar ratio of (*R*)-PVHMA in the PEG-PVH1 and PEG-PVH2 copolymers were about 18.1% and 25.7% according to the peaks area ratio of 4.10 ppm and 6.90–7.80 ppm, respectively.

The (*R*)-PVHMA and PEGMA fragments were respectively hydrophobic and hydrophilic, so the obtained copolymers PEG-PVH were amphiphilic, making them easily disperse in aqueous solution and self-assemble into nanoparticles. PEGMA fragments were affinity with water and stretched into water, while hydrophobic (*R*)-PVHMA fragments were estranged from water and aggregated together which induced fluorescence emission. The stretching PEGMA fragments were considered as a shell and the aggregating (*R*)-PVHMA fragment as a core, so the copolymers were dispersed into aqueous solution as a fluorescent organic nanoparticle (FONs) with a core-shell structure. The TEM image confirmed this result, as shown in Fig. 2(a), where PEG-PVH1 FONs were spherical particles with about 100 nm in diameter,

which also indirectly confirmed the successful combination of the two monomers (*R*)-PVHMA and PEGMA into the copolymers PEG-PVH.

In order to further research the structure of the individual target products OPHT, OPC, HPA, (*R*)-PHMA, (*R*)-PVHMA and PEG-PVH, their FTIR spectra were analyzed and the results were shown in Fig. 2(b). The introduction of octadecyl group into phenothiazine was performed through a simple nucleophilic substitution reaction, and the FTIR spectrum reflected the successful preparation of OPHT because the typical stretching bands of alkanes obviously were presented at 2850 and 2910 cm^{-1} . In the FTIR spectrum of OPC, a vibration band of the introduced $\text{C}=\text{O}$ group evidently appeared at 1690 cm^{-1} , and at the same time, the octadecyl structure remained unchanged. In the curve of HPA, the absorption bands at 2230, 3450 and 2960 cm^{-1} were assigned to the vibration of cyano $\text{C}\equiv\text{N}$, hydroxy $\text{O}-\text{H}$ and alkyl chains, respectively, which implied that the hydrocarbonylation reaction of 4-hydroxyphenylacetonitrile and CHOL was successful. As compared with HPA, the band at 3450 cm^{-1} completely disappeared in the curve of (*R*)-PHMA, while a typical vibration peak of $\text{C}=\text{O}$ group appeared at 1720 cm^{-1} , which indicated that the alcohol hydroxyl groups in the HPA structure were completely depleted and the transesterification reaction between HPA and TFEMA was successful. Moreover, the high enantioselectivity of Novozym435 to the racemic HPA was utilized to realize the construction of intermediate (*R*)-PHMA with *R* configuration. Compared with (*R*)-PHMA, the FTIR spectrum of (*R*)-PVHMA also contained absorption bands at 1720, 2230 and 2960 cm^{-1} , indicating that (*R*)-PVHMA structure contained (*R*)-PHMA fragments. The difference mainly concentrated on the range of 1580–1500 cm^{-1} and 800–750 cm^{-1} , which reflected the stretching vibration and out-of-plane deformation vibration of the conjugated aromatic ring skeleton, respectively. The stretching vibrations of $\text{C}=\text{O}$, $-\text{CH}_2-$ and $\text{C}-\text{O}$ brought about three distinct absorption bands of 1720, 2870 and 1100 cm^{-1} respectively, in the spectrum of the PEG-PVH1 copolymers. The structure of the obtained copolymers included typical characteristics of (*R*)-PVHMA and PEGMA, implying that (*R*)-PVHMA and PEGMA

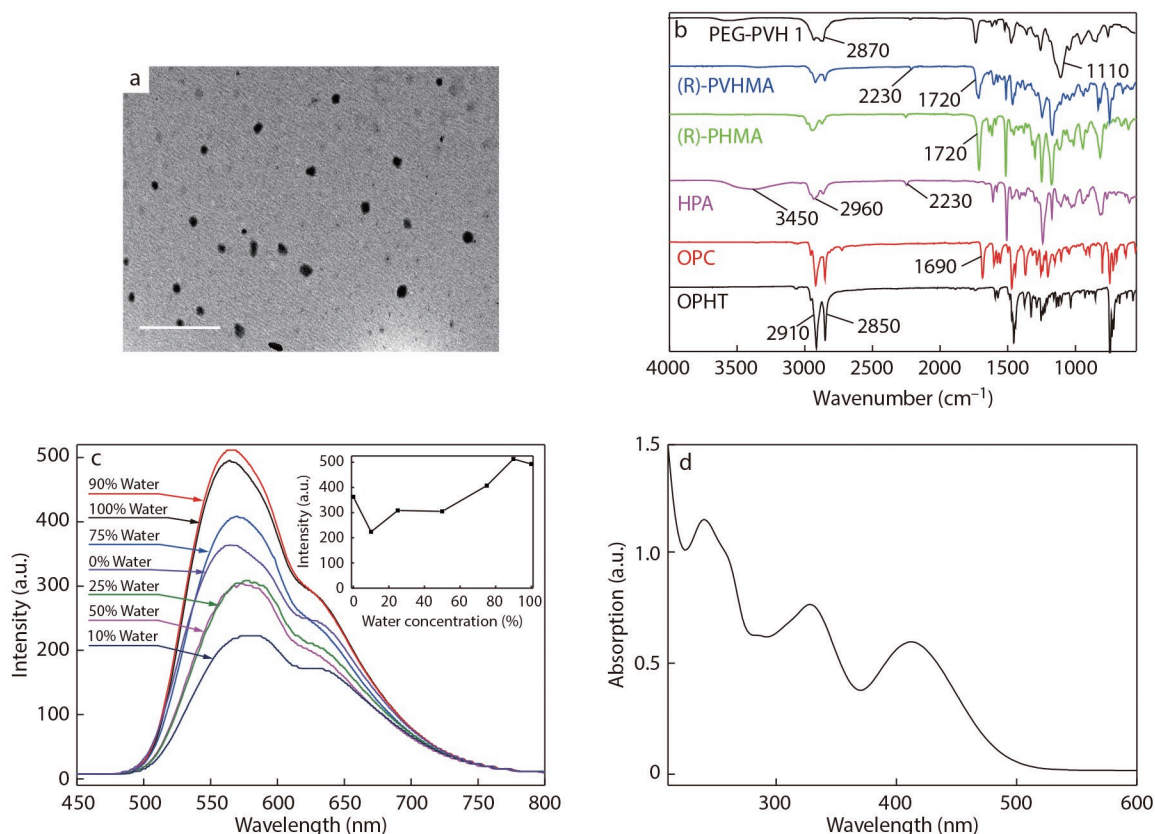


Fig. 2 Characterization of (*R*)-PVHMA monomer and PEG-PVH FONS: (a) TEM image of PEG-PVH dispersed in water, scale bar=1000 nm, (b) FTIR spectra of OPHT, OPC, HPA, (*R*)-PHMA and (*R*)-PVHMA dye monomer and fluorescent copolymers PEG-PVH; (c) fluorescence emission curves of PEG-PVH1 copolymers in the H₂O and THF solution with 405 nm excitation wavelength, and the inset shows the fluorescence intensity of PEG-PVH1 in water solution with different concentrations, and the concentration is about 0.50 mg/mL; (d) UV-Vis spectrum of PEG-PVH1 dispersed in aqueous solution, and the concentration is about 40 μg/mL.

were copolymerized successfully into the PEG-PVH1 copolymers.

The fluorescence curves of PEG-PVH1 dispersed in THF/H₂O solvents with various volume ratios are exhibited in Fig. 2(c). In THF good solvent, the copolymers PEG-PVH1 could emit fluorescence. The reason was that (*R*)-PVHMA had a relatively strong electron-donating ability and formed a D-A structure with a strong electron-withdrawing phenylacetonitrile group, so the intramolecular charge transfer (ICT) effect would emit fluorescence.^[41–43] The fluorescence intensity was slightly reduced when the volume of water was about 10% in the mixed solution, which is caused by a twisted intramolecular charge transfer (TICT) with solvent polarity.^[44] With the volume fraction of H₂O in the mixed solvent continually increasing, the fluorescence intensity gradually increased. In water, the fluorescence intensity showed a very remarkable improvement and the maximum fluorescence wavelength of PEG-PVH1 FONS was about 580 nm with a shoulder peak at 630 nm. The reason was that the copolymers PEG-PVH1 gradually aggregated along with the increase of H₂O fraction in the solution, which hindered the intramolecular motion and activated the restriction of intramolecular motion (RIM), indicating the obvious aggregation-induced emission enhancement (AEE) phenomenon. Amphiphilic copolymers PEG-PVH exhibited self-assemble properties in water, form-

ing corresponding PEG-PVH FONS, whose UV-Vis spectrum was exhibited in Fig. 2(d), where there were three peaks at 240, 330 and 410 nm, respectively. The $\pi \rightarrow \pi^*$ electron transition of polycyclic aromatic rings brought the absorption peak at 240 nm, at the same time, due to the presence of hetero atoms O and N in the molecular structure of the copolymers, the $n \rightarrow \pi^*$ electron transition of their lone electrons resulted in an absorption peak at 330 nm. As mentioned earlier, (*R*)-PVHMA had a relatively strong electron-donating capacity and there was an intramolecular charge transfer between electron-withdrawing groups such as cyano, carbonyl groups and phenothiazine, which led to an absorption peak at 410 nm.^[23]

Moreover, as shown in Fig. 3, the quantum calculations of (*R*)-PVHMA dye and its OPC substrate were achieved from B3LYP/6-31+G(d) method of the Gaussian 09 to investigate the D-A structure on the fluorescence property. For the OPC substrate, most of the electrons mainly concentrate on the aromatic rings in HOMO situation, and they would transfer to -CHO group in LUMO situation, subsequently, these electrons continually transferred to -CN group in LUMO situation of (*R*)-PVHMA dye. As compared with OPC, the more dispersed electrons in LUMO situation of (*R*)-PVHMA would reduce the energy level difference of HOMO and LUMO situations, which was consistent with the fluorescence emission

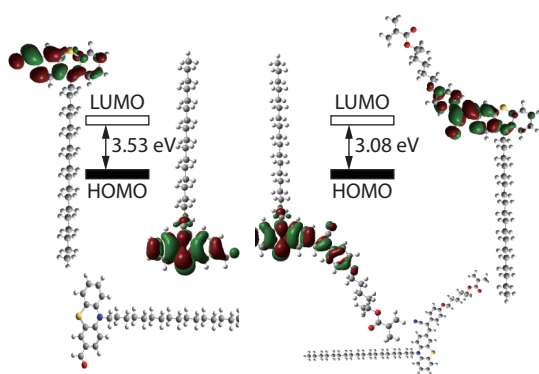


Fig. 3 The quantum calculations of LUMO and HOMO orbits of OPC and (*R*)-PVHMA dyes.

curves as demonstrated in Fig. S3 (in ESI): The emission wavelength of (*R*)-PVHMA transferred from 530 nm to 600 nm of OPC with stronger intensity, and the emission wavelength red-shift of (*R*)-PVHMA dye was very profitable for application in bioimaging area. Otherwise, the PEG-PVH copolymers presented also excellent fluorescence emission in other solvents such as ACN, DCM, DMF and DMSO, as shown in Fig. S4 (in ESI).

The kinetics analysis of RAFT polymerization was further studied in detail. The $^1\text{H-NMR}$ spectra of the samples with various reaction time are exhibited in Fig. S5 (in ESI). The characteristic peaks at 5.61 and 6.17 ppm were attributed to the $-\text{C}=\text{CH}_2$ of PEGMA, and the peaks at 5.56 and 6.13 ppm were attributed to the $-\text{C}=\text{CH}_2$ of (*R*)-PVHMA. Otherwise, the typical peak at 6.80 ppm assigned to trimethylbenzene was selected as interior label, and the conversion rate of PEGMA and (*R*)-PVHMA was calculated by monitoring the intensity change of these peaks mentioned above. From the Fig. S5 (in ESI), it can be observed that the intensity of the above four peaks gradually reduced as the polymerization proceeded, which meant that (*R*)-PVHMA and PEGMA have been gradually used up in polymerization reactions. For 24 h, their conversion rate was about 90% with a high level. The kinetic study of $\ln([M_0]/[M])$ versus time presented a quasilinear first-order procedure as shown in Fig. 4(a). During the polymerization, the conversion rates of (*R*)-PVHMA and

PEGMA remained essentially the same, and the resulted PEG-PVH copolymers should be random copolymers. As shown in Fig. 4(b), during RAFT polymerization, the molecular weights nearly rose linearly with narrow PDI as monomers conversion, indicating a controllable RAFT procedure.

Subsequently, the optical activity of (*R*)-PVHMA fluorescent monomer and its PEG-PVH2 copolymers was investigated. In the transesterification procedure of HPA and TFEMA, the catalyst Novozym435 played a crucial role. Its high enantioselectivity ultimately led to the preferential consumption of the (*R*)-HPA enantiomer, which successfully achieved the transformation from racemate (\pm) HPA to levorotatory (*R*)-PVHMA. The specific rotation $[\alpha]_D^{25^\circ\text{C}}$ of the resulted (*R*)-PVHMA monomer was about -6.39° , and that of PEG-PVH2 copolymers was about -2.96° .

Cytotoxicity and Bioimaging Evaluation of PEG-PVH FONs

L929 cells were used as the reference to evaluate the cytotoxicity of the copolymers PEG-PVH. In the CCK-8 assay, L929 cells were subjected to special treatment: incubation with various concentrations of PEG-PVH1 FONs solution (0, 10, 20, 40, 80, 120 $\mu\text{g}/\text{mL}$) for 8 and 24 h.^[45–48] As exhibited in Fig. 5(a), the cell viability of each experimental group was above 90%, indicating that the prepared PEG-PVH1 FONs have low cytotoxicity and excellent biocompatibility, conferring the potential biomedical applications of the prepared PEG-PVH1 FONs.

Accordingly, the effect of the prepared PEG-PVH1 FONs on cell imaging was also evaluated with L929 cells as the representative, and they were incubated with PEG-PVH1 FONs solution at a concentration of 20 $\mu\text{g}/\text{mL}$.^[49,50] Then, their confocal laser scanning microscope (CLSM) images of experimental cells under 405 nm laser excitation were acquired. As shown in Figs. 5(b)–5(d), the experimental cells showed bright yellow fluorescence under excited light, implying that PEG-PVH1 FONs could readily enter into the cells through endocytosis. On closer inspection, very bright fluorescence could be observed in the periphery of each cell, while the interior was fainter. In the consideration of the sizes of cells, cells cores and PEG-PVH1 FONs, PEG-PVH1 FONs should mainly disperse in the cytoplasmic region after entering the cells. The maxim-

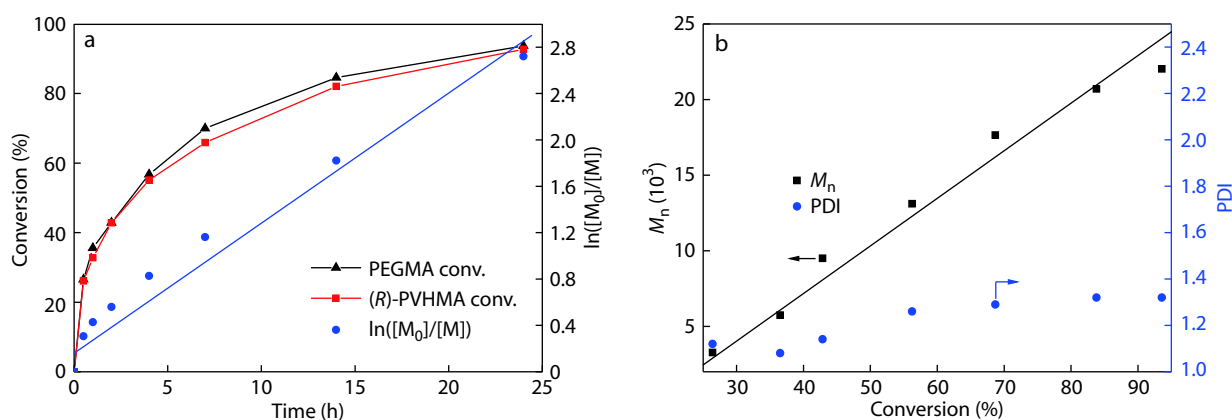


Fig. 4 Kinetics study of PEGMA and PEG-PVH RAFT polymerization: (a) conversion rates and the kinetic analysis of PEG-PVH and PEGMA monomers versus reaction time, (b) the molecular weights and PDI versus monomer conversion.

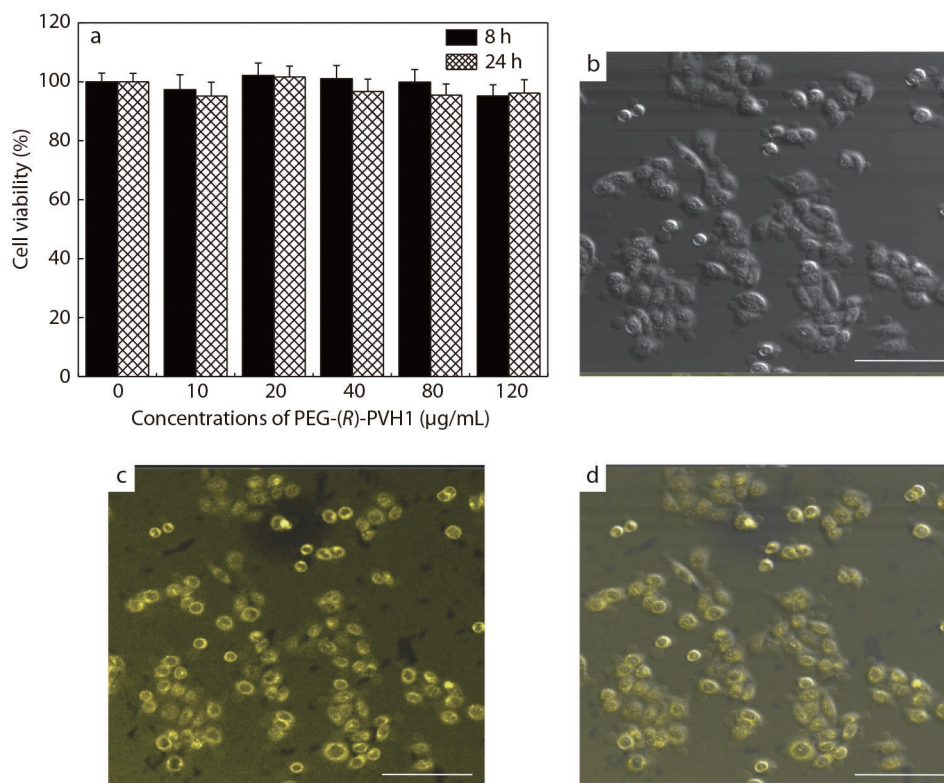


Fig. 5 Biocompatibility estimation and cells imaging of PEG-PVH1 FONs: (a) cell viability of PEG-PVH1 FONs with L929 cells; (b–d) CLSM images of L929 cells incubating with 20 µg/mL of PEG-PVH1 for 3 h at 37 °C, and then fixed with 4% paraformaldehyde for 10 min, (b) bright field, (c) excited by a 405 nm laser, (d) combined image of (b) and (c). Scale bars=100 µm.

um fluorescence emission wavelength tetraphenylethylene skeleton was generally around 470–510 nm, so the imaging performance of PEG-PVH1 FON was better than them owing to red-shift of the emission wavelength. This was because certain molecules or tissues in the organism would fluoresce on their own, which would interfere with the signal during the imaging process, reduce the sensitivity, and affect the imaging effect. The longer fluorescence wavelength of PEG-PVH1 FONs could reduce the background fluorescence of the organism itself to a certain extent, which also meant that the application prospect of PEG-PVH1 FONs in the field of biomedicine was more prospective.

CONCLUSIONS

Due to the strong electron-donating ability of phenothiazine, it was used as an electron donor to construct fluorescent molecules of red light emission with a D-A structure. Based on phenothiazine, a novel (*R*)-PVHMA fluorescent monomer with chirality effect was firstly achieved through enzymatic transesterification. The $[\alpha]_D^{25^\circ\text{C}}$ of the (*R*)-PVHMA was about -6.39° . Afterwards, a series of PEG-PVH1 and PEG-PVH2 copolymers were constructed through RAFT polymerization of (*R*)-PVHMA and PEGMA. When the feed ratio of chiral fluorescent monomer (*R*)-PVHMA increased from 21.5% to 29.6%, the actual (*R*)-PVHMA molar ratio in PEG-PVH increased from 18.1% to 25.7%, and the $[\alpha]_D^{25^\circ\text{C}}$ of PEG-PVH2 copolymers was about -2.96° . The amphiphilic PEG-PVH copolymers self-assembled into nanoparticles in water solution with about

100 nm in diameter. In a 90% water solution of water/THF mixture, the fluorescence intensity reached the maximum, and the fluorescence wavelength of PEG-PVH1 appeared at 580 and 630 nm. The investigation of cytotoxicity and cell uptake shows that PEG-PVH has outstanding biocompatibility and excellent cell imaging effect, and possesses attractive potential in bioimaging application.

Electronic Supplementary Information

Electronic supplementary information (ESI) is available free of charge in the online version of this article at <http://doi.org/10.1007/s10118-021-2596-x>.

ACKNOWLEDGMENTS

This work was financially supported by the Natural Science Foundation of Guangdong Province (Nos. 2018A030313784 and 2021A1515410008), the Colleges and Universities Projects of Guangdong Province (Nos. 2020KTSCX180, 2020KTSCX184 and 2020ZDZX3027), the National Natural Science Foundation of China (No. 51673107) and the Climbing Plan of Guangdong Province (No. PDJH2021a0616).

REFERENCES

- Liang, J.; Kwok, R. T. K.; Shi, H. B.; Tang, B. Z.; Liu, B. Fluorescent light-up probe with aggregation-induced emission

- characteristics for alkaline phosphatase sensing and activity study. *ACS Appl. Mater. Interfaces* **2013**, *5*, 8784–8789.
- Chen, S. J.; Hong, Y. N.; Liu, Y.; Liu, J. Z.; Leung, C. W. T.; Li, M.; Kwok, R. T. K.; Zhao, E. G.; Lam, J. W. Y.; Yu, Y.; Tang, B. Z. Full-range intracellular pH sensing by an aggregation-induced emission-active two-channel ratiometric fluorogen. *J. Am. Chem. Soc.* **2013**, *135*, 4926–4929.
 - Hu, R. R.; Ye, R. Q.; Lam, J. W. Y.; Li, M.; Leung, C. W. T.; Tang, B. Z. Conjugated polyelectrolytes with aggregation-enhanced emission characteristics: synthesis and their biological applications. *Chem. Asian J.* **2013**, *8*, 2436–2445.
 - Liu, L. J.; Liu, W.; Ji, G.; Wu, Z. Y.; Xu, B.; Qian, J.; Tian, W. J. NIR emission nanoparticles based on FRET composed of AIE luminogens and NIR dyes for two-photon fluorescence imaging. *Chinese J. Polym. Sci.* **2019**, *37*, 401–408.
 - Zhi, Y. F.; Li, C.; Song, Z. H.; Yang, Z. J.; Ma, H. W.; Gao, L. C. The location-influenced fluorescence of AIEgens in the microphase-separated structures. *Chinese J. Polym. Sci.* **2019**, *37*, 1060–1064.
 - Qin, W.; Li, K.; Feng, G. X.; Li, M.; Yang, Z. Y.; Liu, B.; Tang, B. Z. Bright and photostable organic fluorescent dots with aggregation-induced emission characteristics for noninvasive long-term cell imaging. *Adv. Funct. Mater.* **2014**, *24*, 635–643.
 - Shi, H. B.; Liu, J. Z.; Geng, J. L.; Tang, B. Z.; Liu, B. Specific detection of integrin $\alpha_v\beta_3$ by light-up bioprobe with aggregation-induced emission characteristics. *J. Am. Chem. Soc.* **2012**, *134*, 9569–9572.
 - Gao, S. J.; Li, Z.; Sun, Z. C.; Wen, J. Y.; Li, F. R.; Du, X. Y.; Liu, Y.; Tian, Y.; Niu, Z. W. Single-wavelength excited ratiometric fluorescence pH probe to image intracellular trafficking of tobacco mosaic virus. *Chinese J. Polym. Sci.* **2020**, *38*, 587–592.
 - Zhao, J. Y.; Peng, J.; Chen, P.; Wang, H. R.; Xue, P. C.; Lu, R. Mechanofluorochromism of difluoroboron β -ketoiminate boron complexes functionalized with benzoxazole and benzothiazole. *Dyes. Pigments* **2018**, *149*, 276–283.
 - Gao, H. Z.; Xu, D. F.; Wang, Y. H.; Zhang, C.; Yang, Y.; Liu, X. L.; Han, A. X.; Wang, Y. Aggregation-induced emission and mechanofluorochromism of tetraphenylbutadiene modified β -ketoiminate boron complexes. *Dyes. Pigments* **2018**, *150*, 165–173.
 - Xue, P. C.; Yao, B. D.; Sun, J. B.; Xu, Q. X.; Chen, P.; Zhang, Z. Q.; Lu, R. Phenothiazine-based benzoxazole derivatives exhibiting mechanochromic luminescence: the effect of a bromine atom. *J. Mater. Chem. C* **2014**, *2*, 3942–3950.
 - Zhan, Y.; Zhao, J. Y.; Peng, Y.; Ye, W. J. Multi-stimuli responsive fluorescent behaviors of a donor- π -acceptor phenothiazine modified benzothiazole derivative. *RSC Adv.* **2016**, *6*, 92144–92151.
 - Xue, P. C.; Ding, J. P.; Chen, P.; Wang, P. P.; Yao, B. Q.; Sun, J. B.; Lu, R. Mechanical force-induced luminescence enhancement and chromism of a nonplanar D-A phenothiazine derivative. *J. Mater. Chem. C* **2016**, *4*, 5275–5280.
 - Li, C. L.; Duan, R. H.; Liang, B. Y.; Han, G. C.; Wang, S. P.; Ye, K. Q.; Liu, Y.; Yi, Y. P.; Wang, Y. Deep-red to near-infrared thermally activated delayed fluorescence in organic solid films and electroluminescent devices. *Angew. Chem. Int. Ed.* **2017**, *56*, 11525–11529.
 - Liu, T. X.; Zhu, L. P.; Zhong, C.; Xie, G. H.; Gong, S. L.; Fang, J. F.; Ma, D. G.; Yang, C. L. Naphthothiadiazole-based near-infrared emitter with a photoluminescence quantum yield of 60% in neat film and external quantum efficiencies of up to 3.9% in nondoped OLEDs. *Adv. Funct. Mater.* **2017**, *27*, 1606384.
 - Zhou, J.; He, B. R.; Xiang, J. Y.; Chen, B.; Lin, G. W.; Luo, W. W.; Lou, X. D.; Chen, S. M.; Zhao, Z. J.; Tang, B. Z. Tuning the AIE activities and emission wavelengths of tetraphenylethene-containing luminogens. *Chem. Select.* **2016**, *1*, 812–818.
 - Xiang, J. Y.; Cai, X. L.; Lou, X. D.; Feng, G. X.; Min, X. H.; Luo, W. W.; He, B. R.; Goh, C. C.; Ng, L. G.; Zhou, J.; Zhao, Z. J.; Liu, B.; Tang, B. Z. Biocompatible green and red fluorescent organic dots with remarkably large two-photon action cross sections for targeted cellular imaging and real-time intravital blood vascular visualization. *ACS Appl. Mater. Interfaces* **2015**, *7*, 14965–14974.
 - Li, Z. H.; Qin, W.; Wu, J. L.; Yang, Z. Y.; Chi, Z. G.; Liang, G. D. Bright electrochemiluminescence films of efficient aggregation-induced emission luminogens for sensitive detection of dopamine. *Mater. Chem. Front.* **2019**, *3*, 2051–2057.
 - Li, L. L.; Li, Y.; Dang, Y. J.; Chen, T. T.; Zhang, A.; Ding, C. Y.; Xu, Z. Imidazole-fused benzothiadiazole-based red-emissive fluorescence probe for lysosomal pH imaging in living cells. *Talanta* **2020**, *217*, 121066.
 - Dhanunjayarao, K.; Sa, S.; Aradhya, B. P. R.; Venkatasubbiah, K. Synthesis of phenanthroimidazole-based four coordinate organoboron compounds. *Tetrahedron* **2018**, *74*, 5819–5825.
 - Jia, J. H.; Cao, K. Y.; Xue, P. C.; Zhang, Y.; Zhou, H. P.; Lu, R. Y-shaped dyes based on triphenylamine for efficient dye-sensitized solar cells. *Tetrahedron* **2012**, *68*, 3626–3632.
 - Yang, X. C.; Lu, R.; Xue, P. C.; Li, B.; Xu, D. F.; Xu, T. H.; Zhao, Y. Y. Carbazole-based organogel as a scaffold to construct energy transfer arrays with controllable fluorescence emission. *Langmuir* **2008**, *24*, 13730–13735.
 - Hua, Y.; Chang, S.; Huang, D. D.; Zhou, X.; Zhu, X. J.; Zhao, J. Z.; Chen, T.; Wong, W. Y.; Wong, W. K. Significant improvement of dye-sensitized solar cell performance using simple phenothiazine-based dyes. *Chem. Mater.* **2013**, *25*, 2146–2153.
 - Sachdeva, T.; Milton, M. D. AIEE active novel red-emitting D- π -A phenothiazine chalcones displaying large Stokes shift, solvatochromism and “turn-on” reversible mechanofluorochromism. *Dyes. Pigments* **2020**, *181*, 108539.
 - Cibotaru, S.; Sandu, A.; Beleu, D.; Marin, L. Water soluble PEGylated phenothiazines as valuable building blocks for bio-materials. *Mater. Sci. Eng. C* **2020**, *116*, 111216.
 - Bai, C. L.; Liu, M. H. From chemistry to nanoscience: not just a matter of size. *Angew. Chem. Int. Ed.* **2013**, *52*, 2678–2683.
 - Wang, Y.; Xu, J.; Wang, Y. W.; Chen, H. Y. Emerging chirality in nanoscience. *Chem. Soc. Rev.* **2013**, *42*, 2930–2962.
 - Goto, H.; Akagi, K. Optically active conjugated polymers prepared from achiral monomers by polycondensation in a chiral nematic solvent. *Angew. Chem. Int. Ed.* **2005**, *44*, 4322–4328.
 - Mallakpour, S.; Zadehnazari, A. Advances in synthetic optically active condensation polymers—a review. *Express. Polym. Lett.* **2011**, *5*, 142–181.
 - Mallakpour, S.; Zeraatpisheh, F.; Sabzalian, M. R. Sonochemical-assisted fabrication of biologically active chiral poly(ester-imide)/TiO₂ bionanocomposites derived from L-methionine and L-tyrosine amino acids. *Express Polym. Lett.* **2011**, *5*, 825–837.
 - Skiba, J.; Kowalczyk, A.; Fik, M. A.; Gapinska, M.; Trzybinski, D.; Wozniak, K.; Vrcek, V.; Czerwiec, R.; Kowalski, K. Luminescent pyrenyl-GNA nucleosides: synthesis, photophysics and confocal microscopy studies in cancer HeLa cells. *Photochem. Photobiol. Sci.* **2019**, *18*, 2449–2460.
 - Zhang, M. X.; Qing, G. Y.; Sun, T. L. Chiral biointerface materials. *Chem. Soc. Rev.* **2012**, *41*, 1972–1984.
 - Deng, M. D.; Li, S.; Cai, L. Z.; Gou, X. J. Preparation of a hydroxypropyl- β -cyclodextrin functionalized monolithic column by one-pot sequential reaction and its applicator for capillary electrochromatographic enantiomer separation. *J. Chromatogr. A* **2019**, *1603*, 269–277.
 - Tan, H. L.; Chen, Q. B.; Chen, T. T.; Liu, H. L. Effects of rigid conjugated groups: toward improving enantioseparation performances of chiral porous organic polymers. *ACS Appl. Mater. Interfaces* **2019**, *11*, 37156–37162.
 - Li, M. M.; Qing, G. Y.; Zhang, M. X.; Sun, T. L. Chiral polymer-based

- biointerface materials. *Sci. China Chem.* **2014**, *57*, 540–551.
- 36 Wrzosek, K.; Harriehausen, I.; Seidel-Morgenstern, A. Combination of enantioselective preparative chromatography and racemization: experimental demonstration and model-based process optimization. *Org. Process. Res. Dev.* **2018**, *22*, 1761–1771.
- 37 Zhang, X. Q.; Chi, Z. G.; Xu, B. J.; Chen, C. J.; Zhou, X.; Zhang, Y.; Liu, S. W.; Xu, J. R. End-group effects of piezofluorochromic aggregation-induced enhanced emission compounds containing distyrylanthracene. *J. Mater. Chem. A* **2012**, *22*, 18505–18513.
- 38 Tao, L.; Liu, J. Q.; Davis, T. P. Branched polymer-protein conjugates made from mid-chain-functional P(HPMA). *Biomacromolecules* **2009**, *10*, 2847–2851.
- 39 Huang, Z. F.; Chen, Y. L.; Zhou, C. Y.; Wang, K.; Liu, X. B.; Mao, L. C.; Yuan, J. Y.; Tao, L.; Wei, Y. Amphiphilic AIE-active copolymers with optical activity by chemoenzymatic transesterification and RAFT polymerization: synthesis, self-assembly and biological imaging. *Dyes. Pigments* **2021**, *184*, 108829.
- 40 Zhang, X. Y.; Zhang, X. Q.; Yang, B.; Liu, M. Y.; Liu, W. Y.; Chen, Y. W.; Wei, Y. Fabrication of aggregation induced emission dye-based fluorescent organic nanoparticles via emulsion polymerization and their cell imaging applications. *Polym. Chem.* **2014**, *5*, 399–404.
- 41 Mei, J.; Hong, Y. N.; Lam, J. W. Y.; Qin, A. J.; Tang, Y. H.; Tang, B. Z. Aggregation-induced emission: the whole is more brilliant than the parts. *Adv. Mater.* **2014**, *26*, 5429–5479.
- 42 Yan, Z. Q.; Yang, Z. Y.; Wang, H.; Li, A. W.; Wang, L. P.; Yang, H.; Gao, B. R. Study of aggregation induced emission of cyano-substituted oligo (*p*-phenylenevinylene) by femtosecond time resolved fluorescence. *Spectrochim. Acta Part A* **2011**, *78*, 1640–1645.
- 43 Qin, W.; Ding, D.; Liu, J. Z.; Yuan, W. Z.; Hu, Y.; Liu, B.; Tang, B. Z. Biocompatible nanoparticles with aggregation-induced emission characteristics as far-red/near-infrared fluorescent bioprobes for *in vitro* and *in vivo* imaging applications. *Adv. Funct. Mater.* **2012**, *22*, 771–779.
- 44 Hu, R. R.; Lager, E.; Aguilar-Aguilar, A.; Liu, J. Z.; Lam, J. W. Y.; Sung, H. H. Y.; Williams, I. D.; Zhong, Y. C.; Wong, K. S.; Pena-Cabrera, E.; Tang, B. Z. Twisted intramolecular charge transfer and aggregation-induced emission of BODIPY derivatives. *J. Phys. Chem. C* **2009**, *113*, 15845–15853.
- 45 Zhang, X. Y.; Hu, W. B.; Li, J.; Tao, L.; Wei, Y. A comparative study of cellular uptake and cytotoxicity of multi-walled carbon nanotubes, graphene oxide, and nanodiamond. *Toxicol. Res.* **2012**, *1*, 62–68.
- 46 Zhao, Y.; Yang, B.; Zhang, Y. L.; Wang, S. Q.; Fu, C. K.; Wei, Y.; Tao, L. Fluorescent PEGylation agent by a thiolactone-based one-pot reaction: a new strategy for theranostic combinations. *Polym. Chem.* **2014**, *5*, 6656–6661.
- 47 Huang, Z. F.; Wang, R. Z.; Chen, Y. L.; Liu, X. B.; Wang, K.; Mao, L. C.; Wang, K.; Yuan, J. Y.; Zhang, X. Y.; Tao, L.; Wei, Y. A polymerizable aggregation-induced emission dye for fluorescent nanoparticles: synthesis, molecular structure and application in cell imaging. *Polym. Chem.* **2019**, *10*, 2162–2169.
- 48 Zhang, X. Y.; Wang, S. Q.; Liu, M. Y.; Hui, J. F.; Yang, B.; Tao, L.; Wei, Y. Surfactant-dispersed nanodiamond: biocompatibility evaluation and drug delivery applications. *Toxicol. Res.* **2013**, *2*, 335–342.
- 49 Zhang, X. Y.; Wang, S. Q.; Fu, C. K.; Feng, L.; Ji, Y.; Tao, L.; Li, S. X.; Wei, Y. PolyPEGylated nanodiamond for intracellular delivery of a chemotherapeutic drug. *Polym. Chem.* **2012**, *3*, 2716–2719.
- 50 Yang, B.; Zhang, Y. L.; Zhang, X. Y.; Tao, L.; Li, S. X.; Wei, Y. Facilely prepared inexpensive and biocompatible self-healing hydrogel: a new injectable cell therapy carrier. *Polym. Chem.* **2012**, *3*, 3235–3238.